Journal of Inorganic Biochemistry 194 (2019) 44–51

Contents lists available at ScienceDirect

Journal of Inorganic Biochemistry

journal homepage: www.elsevier.com/locate/jinorgbio

Interaction of metal ions with tau protein. The case for a metal-mediated tau aggregation

Soha Ahmadi[a,b], Shaolong Zhu[c], Renu Sharma[b], Derek J. Wilson[c,*], Heinz-Bernhard Kraatz[a,b,**]

[a] Department of Chemistry, University of Toronto, 80 St. George Street, Toronto, ON, Canada
[b] Department of Physical and Environmental Science, University of Toronto Scarborough, 1265 Military Trail, Toronto, ON, Canada
[c] Chemistry Department, York University, 4700 Keele Street, Toronto, ON, Canada

ARTICLE INFO

Keywords:
Tau protein
Metalation
Aggregation
Phosphorylation
Reactive oxygen species
Alzheimer's disease

ABSTRACT

Tau protein aggregation and its hyperphosphorylation play an important role in the pathogenesis of Alzheimer's disease. There is also considerable evidence for the accumulation of $Fe^{2/3+}$, Cu^{2+}, and Zn^{2+} in the brain of Alzheimer's patients, although their involvement in the etiology of the disease remains unknown. Here, interactions of the 3d metal ions $Fe^{2/3+}$, Cu^{2+}, and Zn^{2+} with the longest isoform of the human tau protein (htau40) are studied in detail. Electrospray mass spectrometry and ion mobility mass spectrometry analyses confirm the interactions of metal species with tau and that these interactions cause structural changes. Phosphorylation of the full-length htau40 with glycogen synthase kinase 3β (GSK3β), a protein kinase, causes a reduction in metal interactions. Transmission electron microscopy studies of the tau aggregates formed in the presence of metal ions suggest that the presence of metal ions influences the aggregation process. Fluorescence studies of full-length htau40 in the presence of Cu^{2+} indicate the formation of reactive oxygen species, which may contribute further to oxidative stress and neuronal death.

1. Introduction

Since the first report of Alzheimer's disease (AD) in 1906 two main hypotheses have been proposed based on two histopathological hallmarks discovered in the brain of AD patients [1–4]. Extracellular senile plaques (SPs), which are formed from amyloid β (Aβ) aggregation and intracellular neurofibrillary tangles (NFTs), which are the result of tau protein aggregation [5,6].

It is thought that the formation of toxic masses SPs and NFTs contributes to the neuron death. [7–9]

Protein aggregation is a complex multi-step process, and it has been shown that intermediate species, such as abnormal monomers, dimers, and soluble oligomers, are also toxic. Environmental stresses and aging may also contribute or trigger the protein aggregation in the AD [10,11]. Furthermore, the unusual accumulation of transition metals ions copper, iron, and zinc may also be involved in the later stages of AD pathogenesis [12–15]. The interaction of the divalent transition metals Fe^{2+}, Cu^{2+}, and Zn^{2+} ions with Aβ has been widely studied [16–22], significantly less reports focus on their interactions with the tau protein. And while the concentration of free intracellular transition metal ions is negligible as they are tightly controlled in healthy cells, this may change for a diseased state, more likely for a later stage of the pathogenesis AD, in which metal ions may be released. [23–25] Metal dyshomeostasis can lead to the release, with detrimental effects as the metal ions are now able to interact with a range of molecules amongst them intrinsically disordered proteins (IDPs), which may result in their abnormal misfolding and aggregation [26,27]. In the case of Cu and Fe release, this may also result in the formation of reactive oxygen species (ROS). But we want to stress that under the healthy condition the level of metal ions in the brain is tightly controlled [15,28].

The tau protein was discovered by Weingarten and co-workers in 1975, [29] and even though tau mainly presents in neurons an increase in tau concentration in cerebrospinal fluid was reported in pathological condition [30]. Tau is a microtubule-associated protein and is responsible for microtubule (main skeleton of neurons) assembly and stabilization [31–33]. Microtubule assembly of tau is regulated by tau phosphorylation. Abnormal phosphorylation not only disturbs the assembly but also leads to the formation of paired helical filaments (PHFs), which may further aggregate to NFTs [32–35]. There are six isoforms of the tau protein in the human brain, ranging in length from

* Corresponding author.
** Correspondence to: H.-B. Kraatz, Department of Physical and Environmental Science, University of Toronto Scarborough, 1265 Military Trail, Toronto, ON, Canada.
E-mail addresses: dkwilson@yorku.ca (D.J. Wilson), bernie.kraatz@utoronto.ca (H.-B. Kraatz).

https://doi.org/10.1016/j.jinorgbio.2019.02.007
Received 14 November 2018; Received in revised form 5 February 2019; Accepted 10 February 2019
Available online 14 February 2019
0162-0134/ © 2019 Elsevier Inc. All rights reserved.

352 to 441 amino acids [31,33]. These isoforms are categorized based on their microtubule binding domain, which may consist of three (3R) or four (4R) microtubule binding repeats [31,33,36]. Tau is an IDP with a random coil structure with little tendency to aggregate under physiological condition [31,33,35].

It has been shown that copper, iron, and zinc can interact with Aβ [19–21,37–41] and some isoforms of the tau protein [42–48], presumably resulting in irreversible structural changes that may contribute to protein aggregation and/or oxidative stress resulting in further cellular damage. Interaction of Cu^{2+} with Aβ serves as an excellent example, as it has been demonstrated that Cu^{2+} mediates Aβ aggregation by coordination to histidine (His) and that in the presence of Cu^{2+} [16,22,27,49] ROS are formed [40,41]. And we want to make it clear that metal concentrations used in our studies here are not physiologically relevant, but they may offer a glimpse into the interaction of htau40 with these metal ions. Furthermore, we want to make it clear that metal ions are tightly regulated under physiological conditions and that there is no intracellular pool for Cu^{2+} and no free Fe^{3+}. We previously reported the results of an electrochemical study involving the interaction of Cu^{2+}, Zn^{2+}, Fe^{2+} and Fe^{3+} with a shorter isoform of human tau with three binding repeats (htau39), and demonstrated that phosphorylation influences the affinity of metal coordination [47,48]. Furthermore, our results indicated that there are significant differences in the interaction of Fe^{2+} and Fe^{3+} with this particular tau isoform, which has consequences for tau aggregation. While there are a number of studies reporting the interaction of d-block metal ions with tau and some of its fragment peptides [45–47,50–54], the role of these metal on tau aggregation and ROS formation is not well understood.

In this study, we report interactions of $Fe^{2/3+}$, $Cu^{2+,}$ and Zn^{2+} with the full-length htau40, the longest isoform of tau with 441 amino acids (Scheme S1) by mass spectrometry and evaluate the final outcome of the interaction by electron microscopy. In our study, we also include the interaction of these metal ions with phosphorylated tau. We do not embark into studies under conditions that lead to the tau hyperphosphorylation. Our studies indicate that interactions of $Fe^{2/3+}$, $Cu^{2+,}$ and Zn^{2+} with the longest isoform of the human tau protein (htau40) lead to conformational changes, which under our conditions result in tau aggregation, and in the case of Fe^{2+} and Cu^{2+}, ROS formation.

2. Experimental section

2.1. Materials and methods

All chemicals and reagents were analytical grade and obtained from Sigma Aldrich. Human tau40 (htau40) expression was carried out at the Wilson LAB, York University as previously reported (see SI for details). [55,56] Glycogen synthase kinase 3β, active (GSK3β); kinase buffer and 10 mM adenosine triphosphate (ATP) stock solution were purchased from SignalChem (Richmond, Canada). Millipore-Q water (18.2 MΩ cm) was used for sample preparation and all the experiments were performed at room temperature and pH 7.4 unless otherwise mentioned. All metal chloride stock solutions were freshly prepared in Millipore-Q water before the incubation and then diluted to the desire concentration in the buffer. $FeCl_2$ solutions were purged with nitrogen gas for 10 min prior to incubation with the protein in order to reduce the rate of Fe^{2+} oxidation. However, under these conditions, partial oxidation is unavoidable (see UV–vis spectra, Fig. S1). We do not use conditions such as a glovebox to avoid such partial oxidations. We are not implying the presence of free Fe(III) ions under our experimental conditions, as free Fe(III) is stable only under acidic conditions. We did not start the experiments under acidic pH conditions, which would have favoured free Fe(III) and then increase the pH to neutral conditions. Fig. S1 shows the solution prepared from $FeCl_3$ at pH 7.4, which is characterized by a near-UV band near 300 nm tailing into the visible range. This band is due to charge transfer transitions and is typical for colloidal iron(III)-hydroxo species. Full-length htau40 was incubated with excess metal chloride solution at room temperature in order to shift the equilibrium to the metal-tau complex. For aggregation studies a molar ratio of 10:1 M:tau was used, while a molar ratio 5:1 of M:tau was chosen for mass spectrometry experiments to improve the signal to noise ratio. Fluorescence experiments also performed in a molar ratio 5:1 M:tau to minimize the contribution of metal ions in fluorescence intensities.

2.2. Mass spectrometry

Electrospray ionization mass spectrometry (ESI-MS) and ion-mobility spectrometry- electrospray ionization mass spectrometry (IMS-ESI-MS) were performed on Waters Synapt G1 with the following parameters: Capillary 2.5 kV, Sampling Cone 50.0 V, Extraction Cone 1.0 V, Trap Collision Energy 15.0 V, Transfer Collision Energy 6.0 V, ion-mobility spectrometry (IMS) Gas Flow 25.00 mL/min, IMS Wave Velocity 350 m/s, IMS Wave Height 10.0 V. 40 μM htau40 stock solution was desalted and buffer exchanged with ammonium acetate. Then 20 μM htau40 incubated in 0.1 mM $ZnCl_2$, $CuCl_2$, $FeCl_2$ or $FeCl_3$ solution for 1 h. Phosphorylation of htau40 was performed by incubating 80 μM of htau40 in 2.5 μM GSK3β containing in 3 mM ATP in kinase buffer (25 mM Mops (pH 7.2), 12.5 mM β-glycerophosphate, 5.0 mM EGTA, 2.0 mM EDTA, and 25 mM $MgCl_2$) for 2 h at 37 °C. The phosphorylation reaction was stopped by boiling the solution followed by desalting (see the SI for details). The phosphorylated tau solution was incubated in metal solution at the same condition as for native htau40.

2.3. Circular dichroism (CD) spectroscopy

CD measurements were carried out using a Jasco J-815 CD spectrometer (JASCO, Tokyo, Japan) at 25 °C under a constant flow of nitrogen gas. The CD spectra were recorded between 185 and 500 nm using a 0.2 mm quartz cuvette. A solution of htau40 at final concentration of 448 μg/mL with 0.1 mM or without M^{n+} (Cu^{2+}, Zn^{2+}, Fe^{2+} and Fe^{3+}) were prepared. The CD spectrum was recorded for each sample every 15 min for 1 h and after 24 h incubation at room temperature. Each spectrum represents the average of 3 scans.

2.4. Transmission electron microscopy (TEM) experiment

The TEM experiments were performed on a Hitachi H7500 transmission electron microscope using Olympus SIS MegaView II 1.35 MB digital camera and iTEM version 5.2 software. For the TEM experiments, htau40 was incubated with or without M^{n+} (10 μM htau40, 1 mM Cu^{2+}, Zn^{2+}, Fe^{2+} and Fe^{3+} at pH 7.4 for 24 h at room temperature). 5 μL of each solution was placed on carbon-coated copper grids (CF300-Cu, Electron Microscopy Sciences). The grid was allowed to dry at room temperature. Then each grid was stained by adding 5 μL of aqueous uranyl acetate (2%) on it for 1 min. Excess solution was removed using the filter paper.

2.5. Dynamic light scattering (DLS) experiments

The dynamic light scattering (DLS) experiments were performed in a 384-well plate (Corning #3540) using the DynaPro III DLS instrument (Wyatt Technology) at 25 °C. htau40 was incubated for 24 h at room temperature with and without metal chloride solution (10 μM htau40, 0.1 mM M^{n+} in Tris buffer, pH 7.4). A total of 10 acquisitions were performed for each well and the data was processed using DYNAMIC software.

2.6. Fluorescence studies

Fluorescence studies were done with PTi Quantmaster 40 spectrofluorometer using 1 cm quartz cuvette. 2′,7′-dichlorodihydrofluorescein diacetate (H_2DCFDA) will be oxidized to the fluorescent 2′,7′-

dichlorofluorescein (DCF) in the presence of reactive oxygen species (ROS). In order to convert H_2DCFDA to DCF, the de-esterification has been done by employing an alkaline hydrolysis protocol described in the literature [57,58], briefly 500 µL of 1 mM H_2DCFDA solution was added to 2 mL of 0.01 M NaOH. After 30 min, 10 mL of a 25 mM phosphate buffer at pH 7.4 was added to the H_2DCFDA/methanol/NaOH solution. Then this solution was added to the reaction solutions containing 5 µM M^{n+} and 50 µg/mL htau40 to the final concentration of 5 µM DCF. The probe was excited at an excitation wavelength of 490 nm and emission spectrum was recorded in the wavelength range of 500–600 nm. The DCF fluorescence at 523 nm was utilized to monitor the ROS formation upon interaction of M^{n+} with htau40. Control experiments carried out using a solution of a) H_2DCFDA probe alone; b) H_2DCFDA acid with 5 µM M^{n+}, and c) H_2DCFDA with 50 µg/mL htau40.

3. Results and discussion

Interactions of the full-length htau40 with the metal ions Cu^{2+}, Zn^{2+}, Fe^{2+}, and Fe^{3+} were studied in solution at pH 7.4 by circular dichroism (CD) spectroscopy in the range of 185–500 nm. CD spectroscopy is a useful technique to monitor global structural changes that occur as a result of metal complexation and has been applied successfully to the study of the interaction of Fe^{2+}/Fe^{3+} with the shorter isoform htau39 [48]. We previously showed that both $Fe^{2+}$and Fe^{3+} can promote coil-to-helix transition in htau39 after 2 h [48]. The structural changes of htau40 upon Cu^{2+}, Zn^{2+}, Fe^{2+}, and Fe^{3+} incubation were monitored at 25 °C for 1 h (Fig. 1). The CD spectrum of native htau40 under identical conditions was recorded as a control sample, which shows a strong negative signal at 200 nm and a low-intensity negative signal at 288 nm that represent the major random coil and minor tertiary structure, respectively (Fig. S2).

The CD spectrum of htau40 remained virtually unchanged even after 1 h at 25 °C (Fig. S2). However, the addition of M^{n+} to a solution of htau40 caused changes in the intensity of the signals at 200 nm and 288 nm (Fig. 1). Changes of the signal at 200 nm indicate changes in the random coil structure and changes at 288 nm, which represents the aromatic residues and/or cysteine, indicates changes in the tertiary structure of the protein, potentially as the result of metal-tau complexation. While the intensity of the random coil signal decreased upon interaction with Cu^{2+}, the signal intensity increased for other metal ions, which was more significant for Fe^{2+}. There was no evidence for

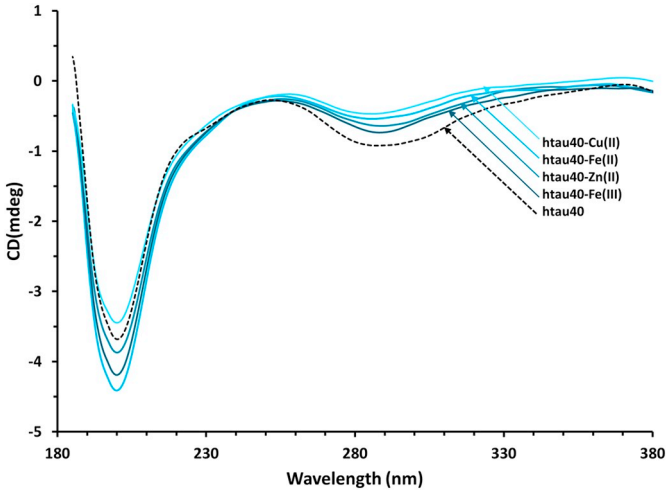

Fig. 1. Monitoring the CD spectrum of htau40 (10 µM, pH 7.4, 25 °C, dashed black line) in the presence of metal salts (0.1 mM M^{n+}, 1 h). Shown are the CD spectra in the absence and presence of Zn^{2+}, Fe^{2+}, Fe^{3+}, and Cu^{2+}. The CD spectra indicate potential changes in the secondary and tertiary structure as a result of metal-htau40 interactions.

the formation of any α-helix or β-sheet structure in the presence of metal ions as we observed for htau39 with $Fe^{2/3+}$ [48]. This observation may suggest that htau40 is more stable than htau39 or has less affinity to interact with $Fe^{2/3+}$. It also emphasizes the role of second microtubule binding repeat, R2 (275–305), in the tau-metal interaction since the only difference between htau40 and htau39 is the presence of R2 in htau40. The CD spectrum also shows that the overall CD intensity at the near-UV region is reduced (Fig. 1), may suggest that the tertiary structure of htau40 is disturbed and the protein is in a more unfolded state, which is more significant for Cu^{2+}. We want to point out that while the CD results suggest a structural change, they do not prove structural change, but CD signals can also be induced as a result of charge transfer bands, such as imidazole to metal. The effect might be significant in the case of Fe(III) (for UV–vis see Fig. S1), and coordination of a putative Fe-hydroxide species (or aggregated Fe-hydroxide) to the protein places it in a chiral environment, resulting in an active CD signal.

And while these changes were subtle, further studies by IMS-ESI-MS indicate a substantial increase in the drift time as a function of added metal ions (see Figs. 2A and S3). This increase in drift time upon M^{n+} interaction suggests that the protein is more unfolded adopting an elliptical shape with a larger collisional cross section.

In order to obtain more information about the tau-metal complex, electrospray ionization mass spectrometry (ESI-MS) studies were carried out. Representative results are shown in Fig. 2B–E, which indicate the formation of polymetallated tau complexes. The number of metal ions coordinated to the protein differs for each of the metal ions. A noticeable difference between the deconvoluted ESI-MS spectrum of native htau40 before and after incubation in the M^{n+} solution (Fig. 2) suggests that M^{n+} binds to htau40. Furthermore, results from the ESI-MS indicate the presence of polymetalation of the protein with more than one metal ion coordinated. While all htau40-M complexes exhibit similar collisional cross sections (Figs. 2A and S3), the average number of metal ions coordinated to the protein is different for each metal ions (Fig. 2B–E; 4 for Cu^{2+}, 5 for Fe^{2+}, 5 for Zn^{2+}, and 7 for Fe^{3+}). Tables S1–S4 list the possible adducts for the major peaks. Notably, the possible adducts upon interaction of Fe^{3+} correspond to species of the type M + 6Fe + 5H, M + 7Fe + 7H, and M + 8Fe + 11H, which indicate metal complexation. Since under the experimental conditions used, Fe (III) hydroxides are present, it is very likely that there is the potential for binding of aggregated Fe-hydroxy clusters. We do not want to imply the coordination of individual Fe(III) ions to the protein. Also note the differences in the ESI-MS results for Fe^{2+} and Fe^{3+}. Calorimetric measurements reported by Mandelkow and co-workers of the interaction of $CuSO_4$ with htau40 (at pH 6.5 and in the presence of 100 mM NaCl) reported a single binding site with a dissociation constant K_d of 0.5 µM [44]. We attribute these differences to differences in experimental conditions (differences in Cu^{2+} source, 100 mM NaCl vs no NaCl – ionic strength, and differences in pH). In addition, metal ions may add non-specifically in the gas phase, which contributes to the observed ESI-MS signal.

Since metalation of htau40 results in a structural change leading to a more unfolded state, we hypothesized that the presence of different metal ions might also affect the final outcome of tau protein aggregation. Our hypothesis is supported by previous studies that showed a more unfolded state is associated with higher aggregation propensity in IDPs [56]. Therefore, transmission electron microscopy (TEM) was used to evaluate the morphological outcome of the aggregation of htau40 with M^{n+} after incubating it for 24 h at room temperature. The presence of metal ions gives rise to the formation of aggregates (Fig. 3 and S4–S8, S4 represent htau40 in the absence of metal ions as control). The exact nature of the aggregates varies for each of the metal ions. While the interaction of Zn^{2+} led to the formation of small globular oligomers (Figs. 3A and S5), the incubation of htau40 with Cu^{2+} led to the formation of larger amorphous aggregates with protofibrils shape branches (Fig. 3B and S6). In the presence of Fe^{3+} small protofibrils were

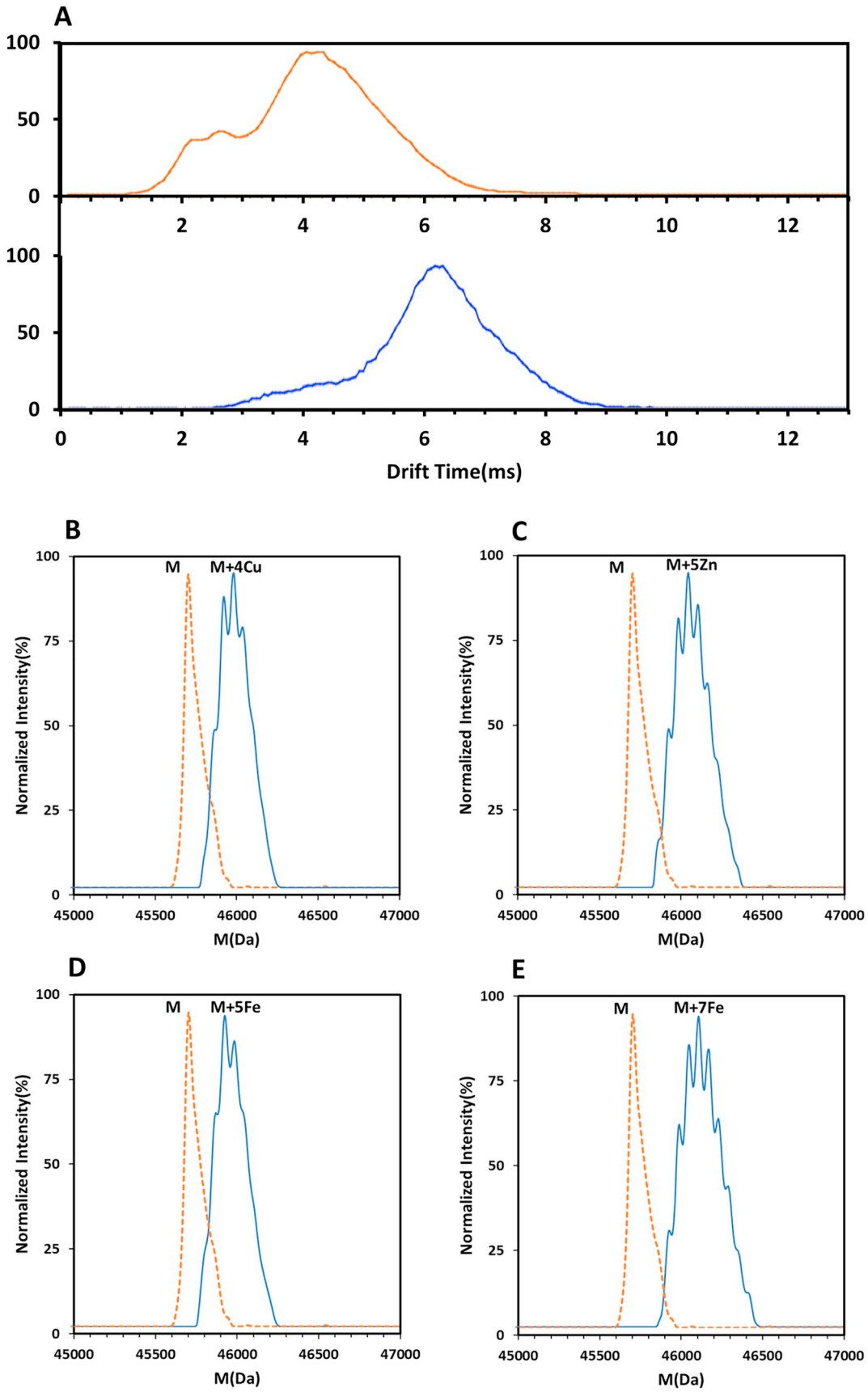

Fig. 2. Interaction of M^{n+} with htau40. IMS-ESI-MS and ESI-MS spectra were recorded after incubation of htau40 with metal ions (20 μM htau40, 0.1 mM M^{n+}, pH 7.4, at 25 °C for 1 h). (A) IMS-ESI-MS drift time distribution plot for native htau40 (upper panel) and in the presence of Cu^{2+} (lower panel). B–E: deconvoluted ESI-MS spectra of native htau40 in the absence (dashed line) and presence of metal ions (solid line): (B) Cu^{2+}, (C) Zn^{2+}, (D) Fe^{2+}, and (E) Fe^{3+}. These studies confirm the interaction of htau40 with M^{n+}, resulting in conformational changes that alter the drift time. Drift time distribution plots for other metal ions are shown in Fig. S3.

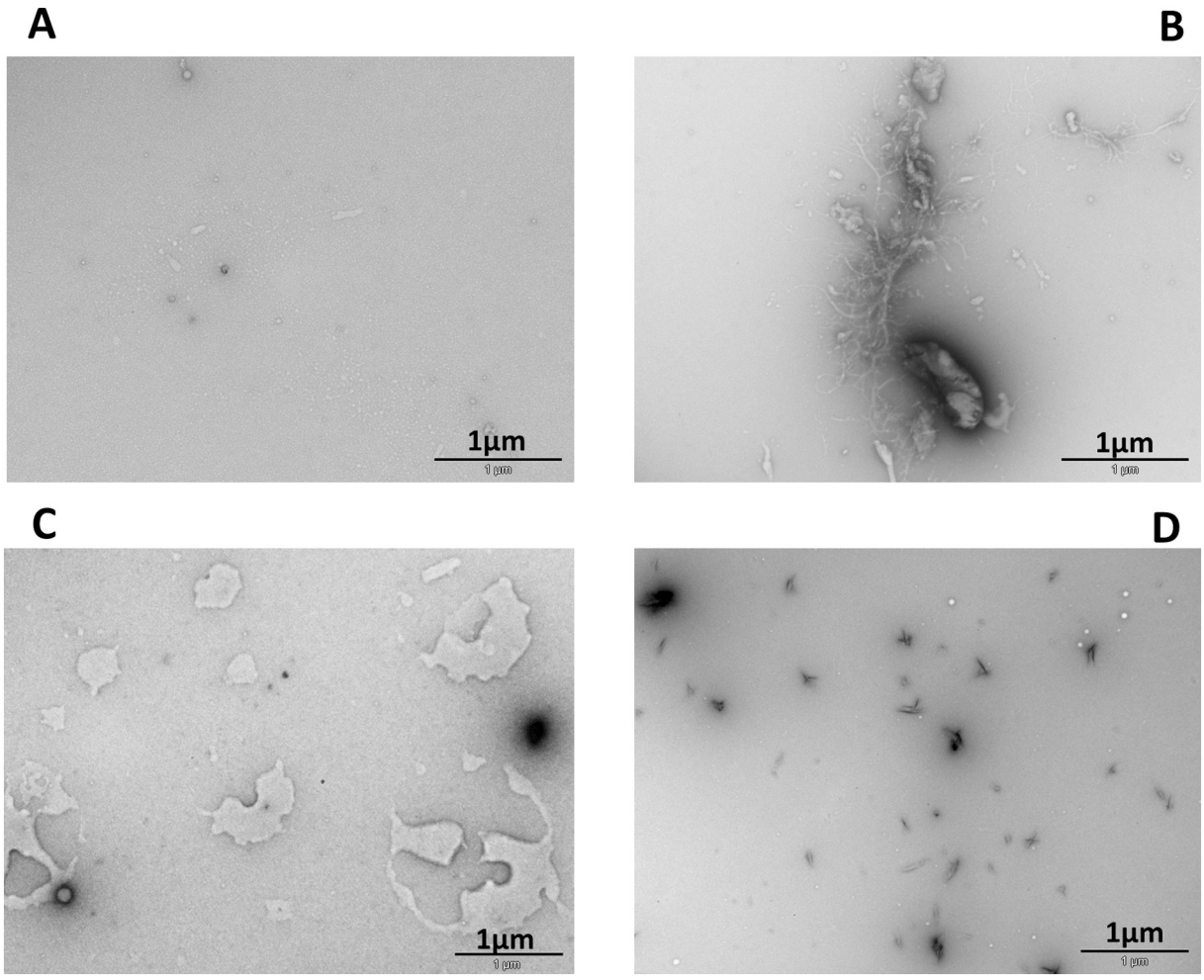

Fig. 3. The effect of M^{n+} on htau40 aggregation. TEM images of htau40 after incubating with (A) Zn^{2+}, (B) Cu^{2+}, (C) Fe^{2+}, and (D) Fe^{3+} (0.1 mM M^{2+}, 10 μM htau40, pH 7.4, room temperature for 24 h). The formation of aggregates suggests that metal ions influence htau40 aggregation. (See Figs. S4–S8 for more TEM images).

formed (Fig. 3D and S8), while in the presence of Fe^{2+} annular structures were formed (Fig. 3C and S7). It is interesting to point that even though, the interaction of htau40 with all M^{n+} studied here gives rise to similar conformational changes after 1 h (Fig. 1, 2A, and S3), their long-term effect on aggregation is completely different for each metal ion (Fig. 3 and S5–S8).

Next, the aggregation of htau40 with metal ions was studied by dynamic light scattering (DLS) under the same conditions used for the TEM studies. DLS provides information about changes in the hydrodynamic radius of proteins as a result of aggregation [59,60]. Earlier reports indicate that the hydrodynamic radius of htau40 in phosphate buffer saline is 4.8–5.4 nm [61]. For the interaction of htau40 with the metal ions, the presence of a htau40 monomer was detected for all samples with an average radius of 5.0 ± 0.4 nm (see Table S5 for the detail) with slightly increase in the polydispersity compare to htau40. But significantly, the size of a larger aggregate is greatly affected by the presence of metal ions showing a clear increase in size from 58.2 ± 7.8 nm to 81.5 ± 10.1 nm after incubating with Cu^{2+}. The results for other metal ions are similar. It is also noteworthy that for Fe^{2+}, an additional signal is observed indicating an average hydrodynamic radius size of 107.8 ± 0.7 nm. In addition, it is also noteworthy that the polydispersity increases as well, indicating a broader size distribution of the aggregate in the presence of metal ions (Table S5). The results obtained by DLS present a picture of the aggregation that is consistent with studies carried out by TEM (vide infra).

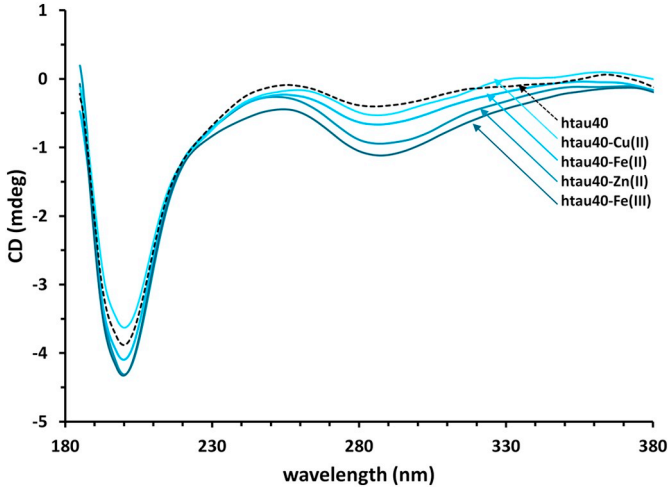

Fig. 4. Monitoring the secondary and tertiary structure of htau40 upon interaction with metal ions (10 M htau40, 0.1 mM M^{n+}, pH 7.4, at 25 °C, 24 h). CD spectra of htau40 after incubation with Zn^{2+}, Fe^{2+}, Fe^{3+}, Cu^{2+}, and without metal ion (dashed line). The CD results indicate that while the random coil structure is maintained, the protein becomes more folded in the presence of M^{n+}.

CD spectrum (Fig. 4) shows that htau40 remains random coil after 24 h incubation in M^{n+}. However, signals at near-UV region slightly shift to the lower wavelength, and their intensity increased (see Table S6). The near-UV CD represents signals associated with the aromatic amino acids side chain (tryptophan, tyrosine, and phenylalanine) and cysteine, which can be affected by the formation of a disulfide bond within the protein [62,63]. There is a total of 3 phenylalanine and 5 tyrosine in htau40 (shown in red in Scheme S1), which may be affected by metal coordination as judged from a shift in near-UV CD signal. Furthermore, enhancement of the CD signal at near UV may suggest that htau40 becomes more folded upon metal interactions, which may be due to the formation of an intramolecular disulfide bond involving the two cysteine residues. Oxidation of cysteine to the corresponding disulfide has been reported for the tau peptide K32 comprising amino acid residues 197–394. NMR studies provide evidence for the formation of an intramolecular disulfide linkage after interaction of Cu^{2+} with this peptide construct [45]. Previous studies of a shorter isoform of tau htau39 demonstrated that Cu^{2+} in the htau39-Cu complex remains redox active [47]. And while surface-bound htau39-$Fe^{2+/3+}$ was redox silent under the reported experimental conditions [48], there is a possibility of metal-mediated ROS formation. Thus, ROS formation upon htau40-M^{n+} interaction was examined exploiting the oxidation of the non-fluorescent 2′,7′-dichlorodihydrofluorescein diacetate (H_2DCFDA) by ROS formed in the reaction to the fluorescent 2′,7′-dichlorofluorescein (DCF).

The increase in fluorescence is the monitored at 523 nm and presented in Fig. 5. DCF is a convenient fluorescence probe that has been widely used for probing ROS under biological conditions [64–67]. Fig. 5 shows the plot of the DCF fluorescence intensity as a function of time for solutions of htau40 in the presence of Fe^{2+}, Fe^{3+}, Zn^{2+}, and Cu^{2+}. The fluorescence intensities of metal ions in the absence of htau40 were subtracted from the htau40-M^{n+} fluorescence intensities. An increase of the fluorescence intensity is observed for htau40 in the presence of Fe^{2+}, Fe^{3+}, and Cu^{2+} as a function of time, and no ROS formation was observed in the presence of Zn^{2+}. The enhancement of the DCF fluorescence intensity is more significant for samples in the presence of Cu^{2+} and Fe^{2+} compared to Fe^{3+}. The differences in the fluorescence profiles of Fe^{2+} and Fe^{3+} emphasize differences in reactivities of the two oxidation states of iron viz. ROS formation, lending further support to the stability of Fe^{2+} under experimental conditions (albeit transient).

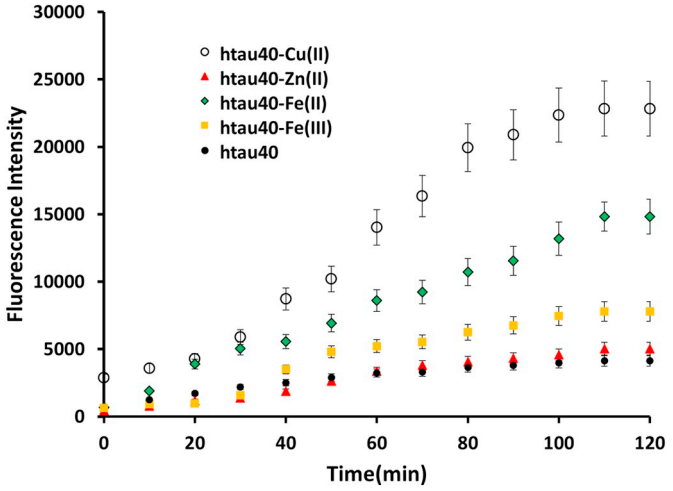

Fig. 5. Time-dependent study of the formation of reactive oxygen species (ROS) due to interactions of 5 μM M^{n+} with 5 μM htau40 using 5 μM DCF. Fluorescence intensity of DCF vs time in the presence of htau40 and Cu^{2+} (circle, o), Zn^{2+} (triangle, Δ) Fe^{2+} (diamond, ♦) and Fe^{3+} (square, □), and without M^{n+} (filled circle, ●) at different time intervals. Samples were scanned every 10 min for a total session of 120 min. The fluorescence intensity of DCF in the presence of M^{n+} was measured as the background for the corresponding metal-htau40 solution. Error bars show the standard deviation of triplicate measurements.

The oxidation of cysteine to cystine by Cu^{2+} is a known reaction in peptides and proteins [46,68]. Su and co-workers studied interaction of Cu^{2+} with R2 (residue 287–304 of htau40) microtubule binding repeat, showing that R2 is oxidized to the corresponding disulfide-bridged dimer in the presence of Cu^{2+}, and hydrogen peroxide can subsequently detected as a result of this redox reaction [46]. Cu^{+} is being formed as a transient, which ultimately is responsible for ROS formation. Likewise, we suggest that for htau40 in the presence of Cu^{2+}, it is a redox reaction involving the proteins Cys residues that enables formation of Cu^{+}, which then gives rise to the observed ROS formation. There are potentially two cysteine in htau40 which may be oxidizable. Likewise it is expected to observe ROS in the presence of Fe(II). The fluorescence assay demonstrates indeed ROS formation in the presence of Fe(II). And while the observed ROS formation is lower than that of Cu^{2+}, which has been observed before for an unrelated system [69], we can speculate that partial oxidation to Fe(III), followed by hydroxide formation will influence the ability of ROS formation. It should be pointed out that formation of Fe(III)-hydroxo cluster at pH 7.4 may reduce the reactivity and availability of Fe(III) for ROS formation [70,71].

Next, we probed the interaction of phosphorylated htau40 (p-htau40) with metal ions. Phosphorylation of htau40 was performed by incubating 80 μM of htau40 in 2.5 μM GSK3β containing 3 mM ATP and 25 mM kinase buffer, pH 7.2 at 37 °C. In order to avoid hyperphosphorylation, reaction was stopped after 2 h. The p-tau was incubated with excess metal ions for 1 h at room temperature before studied by mass spectrometry. Even though we weren't be able to observe completely distinct signals for phosphate adducts by ESI-MS, we were able to assign a doubly phosphorylated tau species in the MS spectrum (see Fig. S9A and Table S7). This is expected given the short incubation time with GSK3β.

The IMS-ESI-MS results clearly show a difference in drift time between native htau40 and p-htau40 (Figs. 1A and 6A). We previously showed by hydrogen/deuterium mass spectrometry that hyperphosphorylated htau40 (with GSK3β) is more unfolded than native htau40 [55,56]. The IMS-ESI-MS drift time distribution plot (Fig. 6A) shows that p-htau40 is also more unfolded compare to the native htau40. The drift time distribution plots confirm that the conformation of p-htau40 changes upon M^{n+} interaction (Fig. 6 and S10). Changes are similar for all metals studied; p-htau40 mainly exist as a unimodal conformational distribution, while after metal addition a bimodal distribution is observable by IMS-ESI-MS.

Interestingly, the ESI-MS spectra (Figs. 5, 7, S9, and S11) show clear differences in the interaction of M^{n+} with p-htau40 as compared to metal interactions with native htau40. The ESI-MS provides evidence for interaction of p-htau40 only with Zn^{2+} resulting on monometalation (Figs. 7 and S9). Table S7 shows the suggested adducts for the interaction of Zn^{2+} with p-htau40. We can speculate that this may be the result of conformational changes upon tau phosphorylation that alter the accessibility of different metal binding sites, or alternatively phosphorylation by GSK3β may have altered the chemical properties of the metal binding sites that could have impacted the binding affinity of different metals.

4. Conclusions

In this study, we investigated the interactions of Fe^{2+}, Fe^{3+}, Cu^{2+}, and Zn^{2+} with native htau40 and phosphorylated htau40. Our results

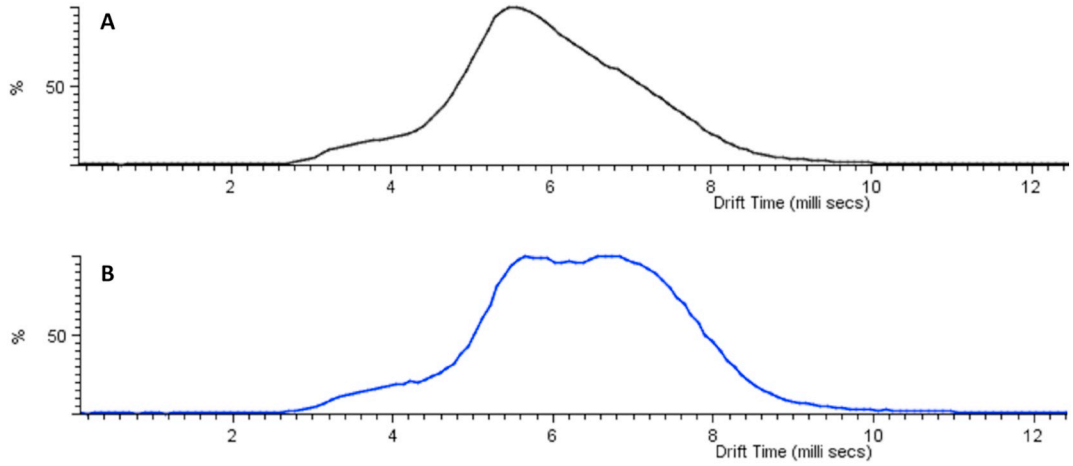

Fig. 6. Interaction of Zn^{2+} with p-htau40. IMS-ESI-MS drift time distribution plot for 20 μM p-htau40 (A) phosphorylated by GSK3β and after 1 h incubating in 0.1 mM Zn^{2+} solution (B) (See Fig. S10 for the drift time distribution plots of other metal ions). The IMS-ESI-MS results show that one dominates conformer for p-htau40 changed to two dominate conformers upon Zn^{2+} interaction. These conformational changes may lead to the p-htau40 aggregation.

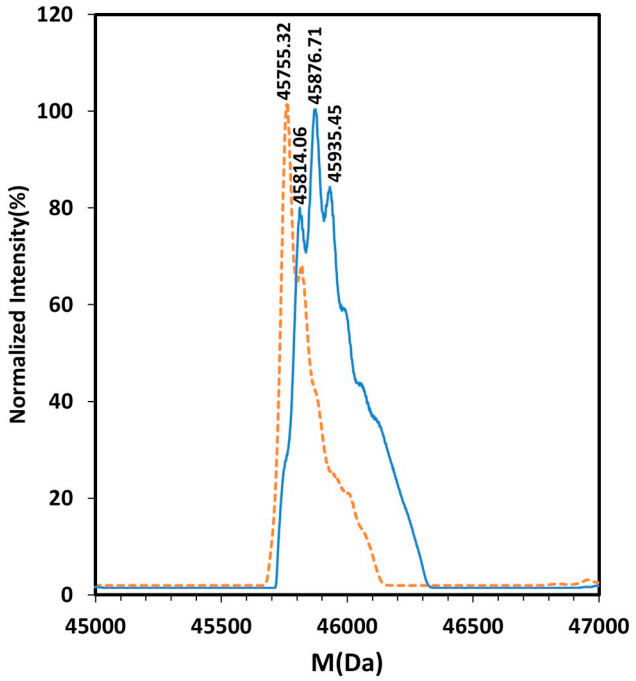

Fig. 7. Interaction of phosphorylated tau with Zn^{2+}. ESI-MS deconvoluted spectra of 20 μM p-htau40 (dashed line) and after incubating in 0.1 mM Zn^{2+} (solid line) for 1 h at room temperature (See Fig. S10 for the ESI-MS deconvoluted spectra of other metal ions). The ESI-MS results confirm complexation of Zn^{2+} with p-htau40. However, compared to native htau40, Zn^{2+} binding to p-htau40 appears to be downregulated (see Table S6 for the possible adducts).

confirm interactions of these metal ions with the tau protein at physiological pH. Polymetalation of the native htau40 results in structural changes that affects the outcome of protein aggregation. The most severe aggregation is observed in the presence of Cu^{2+}, which can be due to the accumulation of two factors: copper complexation and ROS formation. Furthermore, ESI-MS experiments suggest differences in metal affinity as a result of protein phosphorylation. This is an unexpected result. Interestingly, the affinity of Zn^{2+} for htau40 was reduced after phosphorylation with GSK3β, while the interaction between p-htau40 and other metal ions are abrogated which could be attributed to alterations in the binding sites either conformationally or chemically due to phosphates incorporation. These findings emphasize the possible role that metal ions play in the aggregation of tau to form NFs.

Abbreviation

AD	Alzheimer's disease
Aβ	amyloid β
CD	circular dichroism spectroscopy
DCF	2′,7′-dichlorofluorescein
DLS	Dynamic light scattering
ESI-MS	electrospray ionization mass spectrometry
H_2DCFDA	2′,7′-dichlorodihydrofluorescein diacetate
htau40	Longest isoform of human tau protein with four binding repeats
htau39	Human tau with three binding repeats
GSK3β	Glycogen synthase kinase 3β
IMS	ion-mobility spectrometry
IMS-ESI-MS	ion-mobility spectrometry-electrospray ionization mass spectrometry
NFT	neurofibrillary tangle
PD	Polydispersity
p-htau40	phosphorylated htau40
R2	Second microtubule binding repeat of tau protein
ROS	reactive oxygen species
SP	senile plaque
TEM	transmission electron microscopy

Conflicts of interest

There are no conflicts to declare.

Acknowledgements

We gratefully acknowledge funding from NSERC (RGPIN-2016-06122) and financial support from the University of Toronto Scarborough. Access to instrumental facilities in the Department of Chemistry, University of Toronto, and Centre for Research in Mass Spectrometry, York University are appreciated. The authors also acknowledge Robert Temkin for help with TEM experiments and Dr. Greg Wasney, SBC Facility at The Hospital for Sick Children, for help with DLS experiments.

Appendix A. Supplementary data

Supplementary data to this article can be found online at https://doi.org/10.1016/j.jinorgbio.2019.02.007.

References

[1] A. Alzheimer, Neurol. u. Psychiatr. 4 (1911) 356–385, https://doi.org/10.1177/0957154X9100200506.
[2] C. Ballatore, V.M.-Y. Lee, J.Q. Trojanowski, Nat. Rev. Neurosci. 8 (2007) 663–672, https://doi.org/10.1038/nrn2194.
[3] E. Giacobini, G. Gold, Nat. Rev. Neurol. 9 (2013) 677–686, https://doi.org/10.1038/nrneurol.2013.223.
[4] H. Lee, X. Zhu, R.J. Castellani, A. Nunomura, G. Perry, M.A. Smith, J. Pharmacol. Exp. Ther. 321 (2007) 823–829, https://doi.org/10.1124/jpet.106.114009.degenerative.
[5] G.G. Glenner, C.W. Wong, Biochem. Biophys. Res. Commun. 120 (1984) 885–890, https://doi.org/10.1016/S0006-291X(84)80190-4.
[6] C.L. Masters, G. Simms, N.A. Weinman, G. Multhaup, B.L. McDonald, K. Beyreuther, Proc. Natl. Acad. Sci. U. S. A. 82 (1985) 4245–4249, https://doi.org/10.1073/pnas.82.12.4245.
[7] A. Lloret, T. Fuchsberger, E. Giraldo, J. Viña, Free Radic. Biol. Med. 83 (2015) 186–191, https://doi.org/10.1016/j.freeradbiomed.2015.02.028.
[8] A.B. Reiss, H.A. Arain, M.M. Stecker, N.M. Siegart, L.J. Kasselman, Rev. Neurosci. 29 (2018) 613–627, https://doi.org/10.1515/revneuro-2017-0063.
[9] K. Kumar, A. Kumar, R.M. Keegan, R. Deshmukh, Biomed. Pharmacother. 98 (2018) 297–307, https://doi.org/10.1016/j.biopha.2017.12.053.
[10] C.A. Ross, M.A. Poirier, Nat. Rev. Mol. Cell Biol. 6 (2005) 891–898, https://doi.org/10.1038/nrm1742.
[11] C.A. Ross, M.A. Poirier, Nat. Med. 10 (2004) S10–S17, https://doi.org/10.1038/nm1066.
[12] L. Breydo, V.N. Uversky, Metallomics. 3 (2011) 1163–1180, https://doi.org/10.1039/c1mt00106j.
[13] G. Liu, W. Huang, R.D. Moir, C.R. Vanderburg, B. Lai, Z. Peng, R.E. Tanzi, J.T. Rogers, X. Huang, J. Struct. Biol. 155 (2006) 45–51, https://doi.org/10.1016/j.jsb.2005.12.011.
[14] M.A. Greenough, J. Camakaris, A.I. Bush, Neurochem. Int. 62 (2013) 540–555, https://doi.org/10.1016/j.neuint.2012.08.014.
[15] S.S. Leal, H.M. Botelho, C.M. Gomes, Coord. Chem. Rev. 256 (2012) 2253–2270, https://doi.org/10.1016/j.ccr.2012.04.004.
[16] D. Yugay, D.P. Goronzy, L.M. Kawakami, S.A. Claridge, T.-B. Song, Z. Yan, Y.-H. Xie, J. Gilles, Y. Yang, P.S. Weiss, Nano Lett. 16 (2016) 6282–6289, https://doi.org/10.1021/acs.nanolett.6b02590.
[17] K.I. Silva, B.C. Michael, S.J. Geib, S. Saxena, J. Phys. Chem. B 118 (2014) 8935–8944, https://doi.org/10.1021/jp500767n.
[18] V.W. Hung, H. Masoom, K. Kerman, J. Electroanal. Chem. 681 (2012) 89–95, https://doi.org/10.1016/j.jelechem.2012.05.023.
[19] C.-J. Lin, H.-C. Huang, Z.-F. Jiang, Brain Res. Bull. 82 (2010) 235–242, https://doi.org/10.1016/j.brainresbull.2010.06.003.
[20] P. Faller, ChemBioChem. 10 (2009) 2837–2845, https://doi.org/10.1002/cbic.200900321.
[21] S. Bolognin, L. Messori, D. Drago, C. Gabbiani, L. Cendron, P. Zatta, Int. J. Biochem. Cell Biol. 43 (2011) 877–885, https://doi.org/10.1016/j.biocel.2011.02.009.
[22] C.D. Syme, R.C. Nadal, S.E.J. Rigby, J.H. Viles, J. Biol. Chem. 279 (2004) 18169–18177, https://doi.org/10.1074/jbc.M313572200.
[23] M. Schrag, C. Mueller, U. Oyoyo, M.A. Smith, W.M. Kirsch, Prog. Neurobiol. 94 (2011) 296–306, https://doi.org/10.1016/j.pneurobio.2011.05.001.
[24] A.I. Bush, Curr. Opin. Chem. Biol. 4 (2000) 184–191, https://doi.org/10.1016/S1367-5931(99)00073-3.
[25] K.J. Barnham, A.I. Bush, Chem. Soc. Rev. 43 (2014) 6727–6749, https://doi.org/10.1039/C4CS00138A.
[26] P. Faller, C. Hureau, Dalton Trans. (2009) 1080–1094, https://doi.org/10.1039/B813398K.
[27] P. Faller, C. Hureau, G. La Penna, Acc. Chem. Res. 47 (2014) 2252–2259, https://doi.org/10.1021/ar400293h.
[28] C. Hureau, Coord. Chem. Rev. 256 (2012) 2164–2174, https://doi.org/10.1016/j.ccr.2012.03.037.
[29] M.D. Weingarten, A.H. Lockwood, S.-Y. Hwo, M.W. Kirschner, Proc. Natl. Acad. Sci. U. S. A. 72 (1975) 1858–1862, https://doi.org/10.1073/pnas.72.5.1858.
[30] B. Liu, B. Poolman, A.J. Boersma, ACS Chem. Biol. 12 (2017) 2510–2514, https://doi.org/10.1021/acschembio.7b00348.
[31] Y. Wang, E. Mandelkow, Nat. Rev. Neurosci. 17 (2016) 5–21, https://doi.org/10.1038/nrn.2015.1.
[32] L. Buée, T. Bussière, V. Buée-Scherrer, A. Delacourte, P.R. Hof, Brain Res. Rev. 33 (2000) 95–130, https://doi.org/10.1016/S0165-0173(00)00019-9.
[33] T. Guo, W. Noble, D.P. Hanger, Acta Neuropathol. 133 (2017) 665–704, https://doi.org/10.1007/s00401-017-1707-9.
[34] G.V.W. Johnson, W.H. Stoothoff, J. Cell Sci. 117 (2004) 5721–5729, https://doi.org/10.1242/jcs.01558.
[35] S. Jeganathan, M. Von Bergen, E.-M. Mandelkow, E. Mandelkow, Biochemistry. 47 (2008) 10526–10539, https://doi.org/10.1021/bi800783d.
[36] H. Kadavath, R.V. Hofele, J. Biernat, S. Kumar, K. Tepper, H. Urlaub, E. Mandelkow, M. Zweckstetter, Proc. Natl. Acad. Sci. 112 (2015) 7501–7506, https://doi.org/10.1073/pnas.1504081112.
[37] G. Drochioiu, M. Manea, M. Dragusanu, M. Murariu, E.S. Dragan, B.A. Petre, G. Mezo, M. Przybylski, Biophys. Chem. 144 (2009) 9–20, https://doi.org/10.1016/j.bpc.2009.05.008.
[38] P.D.Q. Huy, Q. Van Vuong, G. La Penna, P. Faller, M.S. Li, ACS Chem. Neurosci. 7 (2016) 1348–1363, https://doi.org/10.1021/acschemneuro.6b00109.
[39] P. Faller, C. Hureau, O. Berthoumieu, Inorg. Chem. 52 (2013) 12193–12206, https://doi.org/10.1021/ic4003059.
[40] C. Cheignon, F. Collin, P. Faller, C. Hureau, Dalton Trans. 45 (2016) 12627–12631, https://doi.org/10.1039/C6DT01979J.
[41] C. Cheignon, M. Jones, E. Atrián-Blasco, I. Kieffer, P. Faller, F. Collin, C. Hureau, Chem. Sci. 8 (2017) 5107–5118, https://doi.org/10.1039/C7SC00809K.
[42] Y. Huang, Z. Wu, Y. Cao, M. Lang, B. Lu, B. Zhou, Cell Rep. 8 (2014) 831–842, https://doi.org/10.1016/j.celrep.2014.06.047.
[43] J.-Y. Hu, D.-L. Zhang, X.-L. Liu, X.-S. Li, X.-Q. Cheng, J. Chen, H.-N. Du, Y. Liang, Biochim. Biophys. Acta, Mol. Basis Dis. 1863 (2017) 414–427, https://doi.org/10.1016/j.bbadis.2016.11.022.
[44] L.M. Sayre, G. Perry, P.L.R. Harris, Y. Liu, K.A. Schubert, M.A. Smith, J. Neurochem. 74 (2000) 270–279, https://doi.org/10.1046/j.1471-4159.2000.0740270.x.
[45] A. Soragni, B. Zambelli, M.D. Mukrasch, J. Biernat, S. Jeganathan, C. Griesinger, S. Ciurli, E. Mandelkow, M. Zweckstetter, Biochemistry 47 (2008) 10841–10851, https://doi.org/10.1021/bi8008856.
[46] X.-Y. Su, W.-H. Wu, Z.-P. Huang, J. Hu, P. Lei, C.-H. Yu, Y.-F. Zhao, Y.-M. Li, Biochem. Biophys. Res. Commun. 358 (2007) 661–665, https://doi.org/10.1016/j.bbrc.2007.04.191.
[47] S. Martic, M.K. Rains, H.-B. Kraatz, Anal. Biochem. 442 (2013) 130–137, https://doi.org/10.1016/j.ab.2013.07.015.
[48] S. Ahmadi, I.I. Ebralidze, Z. She, H.-B. Kraatz, Electrochim. Acta 236 (2017) 384–393, https://doi.org/10.1016/j.electacta.2017.03.175.
[49] W.A. Gunderson, J. Hernández-Guzmán, J.W. Karr, L. Sun, V.A. Szalai, K. Warncke, J. Am. Chem. Soc. 134 (2012) 18330–18337, https://doi.org/10.1021/ja306946q.
[50] L.-X. Zhou, J.-T. Du, Z.-Y. Zeng, W.-H. Wu, Y.-F. Zhao, K. Kanazawa, Y. Ishizuka, T. Nemoto, H. Nakanishi, Y.-M. Li, Peptides. 28 (2007) 2229–2234, https://doi.org/10.1016/j.peptides.2007.08.022.
[51] Q. Ma, Y. Li, J. Du, H. Liu, K. Kanazawa, T. Nemoto, H. Nakanishi, Y. Zhao, Peptides. 27 (2006) 841–849, https://doi.org/10.1016/j.peptides.2005.09.002.
[52] Q.-F. Ma, Y.-M. Li, J.-T. Du, K. Kanazawa, T. Nemoto, H. Nakanishi, Y.-F. Zhao, Biopolymers. 79 (2005) 74–85, https://doi.org/10.1002/bip.20335.
[53] X. Du, Y. Zheng, Z. Wang, Y. Chen, R. Zhou, G. Song, J. Ni, Q. Liu, Inorg. Chem. 53 (2014) 11221–11230, https://doi.org/10.1021/ic501788v.
[54] K. Voss, C. Harris, M. Ralle, M. Duffy, C. Murchison, J.F. Quinn, Transl. Neurodegener. 3 (2014) 24, https://doi.org/10.1186/2047-9158-3-24.
[55] S. Zhu, J.L. Campbell, I. Chernushevich, J.C.Y. Le Blanc, D.J. Wilson, J. Am. Soc. Mass Spectrom. 27 (2016) 991–999, https://doi.org/10.1007/s13361-016-1364-6.
[56] S. Zhu, A. Shala, A. Bezginov, A. Sljoka, G. Audette, D.J. Wilson, PLoS One 10 (2015) e0120416, , https://doi.org/10.1371/journal.pone.0120416.
[57] C.A. Cohn, S.R. Simon, M.A. Schoonen, Part. Fibre Toxicol. 5 (2008) 2, https://doi.org/10.1186/1743-8977-5-2.
[58] C.P. LeBel, H. Ischiropoulos, S.C. Bondy, Chem. Res. Toxicol. 5 (1992) 227–231, https://doi.org/10.1021/tx00026a012.
[59] E. Akoury, M. Gajda, M. Pickhardt, J. Biernat, P. Soraya, C. Griesinger, E. Mandelkow, M. Zweckstetter, J. Am. Chem. Soc. 135 (2013) 2853–2862, https://doi.org/10.1021/ja312471h.
[60] B. Lorber, F. Fischer, M. Bailly, H. Roy, D. Kern, Biochem. Mol. Biol. Educ. 40 (2012) 372–382, https://doi.org/10.1002/bmb.20644.
[61] M. Von Bergen, S. Barghorn, S. Jeganathan, E.M. Mandelkow, E. Mandelkow, Neurodegener. Dis. 3 (2006) 197–206, https://doi.org/10.1159/000095257.
[62] S.M. Kelly, N.C. Price, Curr. Protein Pept. Sci. 1 (2000) 349–384.
[63] S.R. Martin, M.J. Schilstra, L. Wilson, P. Tran (Eds.), Methods Cell Biol. Vol 84, Academic Press, 2008, pp. 263–293, , https://doi.org/10.1016/S0091-679X(07)84010-6.
[64] S.G. Rhee, T.-S. Chang, W. Jeong, D. Kang, Mol. Cell 29 (2010) 539–549, https://doi.org/10.1007/s10059-010-0082-3.
[65] R.P. Rastogi, S.P. Singh, D.-P. Häder, R.P. Sinha, Biochem. Biophys. Res. Commun. 397 (2010) 603–607, https://doi.org/10.1016/j.bbrc.2010.06.006.
[66] X. Chen, Z. Zhong, Z. Xu, L. Chen, Y. Wang, Free Radic. Res. 44 (2010) 587–604, https://doi.org/10.3109/10715761003709802.
[67] C.P. LeBel, H. Ischiropoulos, S.C. Bondy, Chem. Res. Toxicol. 5 (1992) 227–231, https://doi.org/10.1021/tx00026a012.
[68] D. Choi, A.A. Alshahrani, Y. Vytla, M. Deeconda, V.J. Serna, R.F. Saenz, L.A. Angel, J. Mass Spectrom. 50 (2015) 316–325, https://doi.org/10.1002/jms.3530.
[69] E. Gammella, S. Recalcati, G. Cairo, Oxidative Med. Cell. Longev. 2016 (2016) 8629024, , https://doi.org/10.1155/2016/8629024.
[70] B. D'Autréaux, M.B. Toledano, Nat. Rev. Mol. Cell Biol. 8 (2007) 813–824, https://doi.org/10.1038/nrm2256.
[71] R. Mittler, Trends Plant Sci. 22 (2017) 11–19, https://doi.org/10.1016/j.tplants.2016.08.002.